

# Biodynamic Response and Spinal Load Estimation of Seated Body in Vibration Using Finite Element Modeling

Wenping WANG<sup>1</sup>, Babak BAZRGARI<sup>2</sup>, Aboufazel SHIRAZI-ADL<sup>1\*</sup>,  
Subhash RAKHEJA<sup>3</sup> and Paul-Émile BOILEAU<sup>4</sup>

<sup>1</sup>Department of Mechanical Engineering, Ecole Polytechnique, C.P. 6079, Succ centre-ville, Montreal, Quebec, H3C 3A7, Canada

<sup>2</sup>Department of Industrial and Systems Engineering, Virginia Tech., USA

<sup>3</sup>Department of Mechanical Engineering, Concordia University, Montreal, Canada

<sup>4</sup>Institut de recherche Robert-Sauvé en santé et en sécurité du travail, Montreal, Canada

*Received June 5, 2009 and accepted May 6, 2010*

**Abstract:** Trunk biomechanical models play an indispensable role in predicting muscle forces and spinal loads under whole-body vibration (WBV) exposures. Earlier measurements on the force-motion biodynamic response (impedance, apparent mass) at the body-seat interface and vibration transmissibility (seat to head) have led to the development of different mechanical models. Such models could simulate the overall passive response and serve as an important tool for vehicle seat design. They cannot, however, evaluate physiological parameters of interest under the WBV. On the contrary, anatomical models simulating human's physiological characteristics can predict activities in muscles and their dynamic effects on the spine. In this study, a kinematics-driven nonlinear finite element model of the spine, in which the kinematics data are prescribed, is used to analyse the trunk response in seated WBV. Predictions of the active model (i.e., with varying muscle forces) as compared with the passive model (i.e., with no muscle forces) compared satisfactorily with measurements on vertical apparent mass and seat-to-head transmissibility biodynamic responses. Results demonstrated the crucial role of muscle forces in the dynamic response of the trunk. Muscle forces, while maintaining trunk equilibrium, substantially increased the compression and shear forces on the spine and, hence, the risk of tissue injury.

**Key words:** Seated-body vibration, Biodynamic responses, Finite element modelling, Spinal loads, Muscle forces

## Introduction

Low back pain (LBP) is a major musculoskeletal disorder with substantial human suffering and economic costs. Prolonged exposure to whole-body vibration (WBV) is recognized as a risk factor for spine disorders<sup>1, 2)</sup> even though underlying mechanisms for such an association remain yet to be identified. Proper injury prevention and treatment programs require a sound knowledge of trunk muscle forces and spinal loads under WBV exposure. Since these loads cannot be measured directly and non-invasively, biomechanical models remain as a viable tool with the potential to play an indispensable role in spine pathomechanics.

Earlier measurements on the force-motion biodynamic response (impedance, apparent mass) at the body-seat interface and vibration transmissibility (seat to head) have led to the development of different mechanical-equivalent models<sup>3, 4)</sup>. Such models could simulate the overall passive biodynamic responses under various vibration and postural conditions and

as such serve as an important tool in vehicle seat design. They are, however, not applicable for the prediction of physiological parameters of the seated body such as the musculoskeletal loading during the WBV exposure. On the contrary, the anatomical-based models that incorporate both active and passive components of the trunk could not only accurately simulate human's physiological characteristics but also provide a reliable estimation of muscle forces and spinal loads that are hardly amenable to direct measurements. Finite element (FE) models offer the potential to accurately representing these active and passive components under various WBV environments<sup>5)</sup>. The existing FE models of the human trunk under WBV, however, are mostly limited either to the simulation of the passive responses alone neglecting muscle activation<sup>6)</sup> or using deterministic approach to incorporate active muscle forces<sup>7)</sup>. Time-varying activations in muscles could substantially influence the trunk biodynamics while maintaining equilibrium and stability. The experimental biodynamic data on apparent mass (APMS) and vibration transmissibility collected during studies on the movements of the body during exposure to WBV and/or shock remain naturally of crucial significance for the validation of lumped-parameter mechanical-equivalent as

\*To whom correspondence should be addressed.  
E-mail: abshir@meca.polymtl.ca

well as FE biodynamic models.

A two-dimensional FE model of the spine, viscera, head, pelvis and buttocks in the mid-sagittal plane, developed by Kitazaki and Griffin<sup>6</sup>, was used to predict the passive physical responses of the seated upper body. The model was validated by comparison of its predictions in modal analyses with measurements. This model showed reasonably good agreement with the measured apparent mass and seat-to-head transmissibility data in the range of 0 to 10 Hz. Pankoke *et al.*<sup>7</sup> introduced a simplified version of the human FE model, originally developed by Buck and Wölfel<sup>8</sup>, for the purpose of computing spinal loads at lower lumbar levels under applied static (including a constant extensor muscle force that depended on the posture) and dynamic loads. The model validation was based on the mechanical impedance and transmissibility from the seat to the L4 and head. This model predicted the measured impedance response reasonably well under vertical vibration at frequencies below 6 Hz but the response deviated from the measured data at higher frequencies. The model responses in terms of transmissibility from the seat to the L4 and head revealed reasonably good estimations of the resonance frequency but overestimated the amplification at resonance frequency. Hinz *et al.*<sup>9</sup> extended an earlier FE model<sup>10</sup> to predict static and dynamic compression and shear forces arising from the posture and whole-body vibration exposure. This FE model was validated based on the apparent mass data from the Federal Institute for Occupational Safety and Health (FIOOSH) and partners in the frequency range up to 20 Hz. Seidel *et al.*<sup>11</sup> further developed a set of FE models based on human anatomy to estimate intraspinal forces at all lumbar levels accounting for real exposure conditions. These models were adapted to typical postures of European drivers and their anthropometric parameters. Although these models employed a detailed representation of the trunk muscles, the dynamic effect of muscle forces was not revealed, neither was the validation of the model discussed.

In this study, an existing validated nonlinear FE model accounting for both nonlinear passive properties of the ligamentous spine and a detailed musculature with time-varying unknown muscle forces while prescribing kinematics data<sup>12–15</sup> is validated using measured vertical apparent mass and seat-to-head transmissibility biodynamic responses<sup>16, 17</sup>. The effects of muscle activation on the biodynamic responses are investigated by comparison of estimations with those obtained employing the passive model alone with no muscle activation. Furthermore, this kinematics-driven model is used to evaluate the effect of muscle forces on spinal loads during the WBV. The results are hypothesized to demonstrate the crucial role of muscle forces on biodynamic response and spinal loads in seated whole body vibrations.

## Methods

### FE model

An anatomical model of the human trunk is employed in this study (see Fig. 1). The FE model is made of six nonlinear deformable beams representing T12–S1 spinal motion segments, seven rigid elements for lumbosacral vertebrae (L1–S1) and head–T12 (as a single body) as well as a connector element to simulate the buttock-seat interface<sup>12–15</sup>.

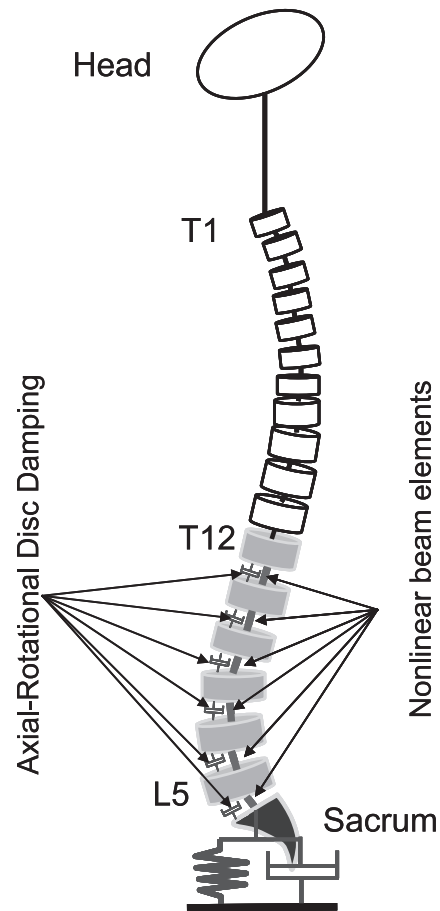


**Fig. 1.** Overall schematic representation of the human trunk in the finite element model (sagittal plane is shown here with the S1 and L1 vertebrae located just below the L5 and T12 vertebrae, respectively).

The beam elements represent the overall nonlinear stiffness of T12–S1 motion segments (i.e., vertebrae, disk, facets and ligaments) at different levels with nonlinear axial compression–strain and sagittal/lateral/axial moment–rotation relations defined in earlier studies<sup>18</sup>. Inter-segmental translational and rotational damping coefficients employ the measured values<sup>18</sup> with translational damping (1,200 Ns/m) and angular damping (1.2 Nms/rad). Mass and mass moments of inertia of trunk/head/arms/pelvis are distributed at different levels along the spine at their corresponding gravity centres, see Table 1<sup>19</sup>.

The current sagittally symmetric model incorporates a detailed trunk musculature which includes 46 local (attached to the lumbar vertebrae) and 10 global (attached to the thoracic cage) muscles<sup>20, 21</sup>, as illustrated in Fig. 2. Each muscle is represented by a single fascicle inserted into the center of its attachment areas. A kinematics-driven approach is employed to evaluate trunk muscle forces subject to prescribed kinematics and external loads (additional details are available elsewhere<sup>12–15, 22–24</sup>). This approach employs available measured kinematics data to generate additional equilibrium equations at each level in order to alleviate the kinetic redundancy of the problem. The redundancy is due to the large number of

**Table 1. Mass, mass moment of inertia and corresponding location of mass centres at different trunk levels in the FE model<sup>19)</sup>**

| Level     | % TM | % BM    | I <sub>xx</sub> | I <sub>yy</sub> | I <sub>zz</sub> | CG - z | CG - x |
|-----------|------|---------|-----------------|-----------------|-----------------|--------|--------|
| Head      | —    | 6.94    | 27.18           | 29.34           | 20.13           | 597.60 | -10.00 |
| Upper Arm | —    | 2 × 2.8 | 12.63           | 11.30           | 3.80            | 447.38 | 30.00  |
| Lower arm | —    | 2 × 1.6 | 6.45            | 5.99            | 1.20            | 426.85 | 30.00  |
| Hand      | —    | 2 × 0.6 | 1.31            | 0.88            | 0.50            | 405.81 | 30.00  |
| T1        | 3.59 | 1.28    | 6.70            | 2.00            | 8.70            | 467.60 | -8.00  |
| T2        | 3.88 | 1.38    | 3.40            | 2.40            | 9.10            | 447.38 | -12.00 |
| T3        | 4.15 | 1.47    | 8.40            | 3.20            | 11.50           | 426.85 | -20.00 |
| T4        | 4.46 | 1.58    | 8.30            | 3.40            | 11.70           | 405.81 | -28.00 |
| T5        | 4.72 | 1.68    | 8.00            | 3.50            | 11.50           | 384.14 | -33.00 |
| T6        | 5.03 | 1.78    | 7.80            | 3.90            | 11.60           | 361.70 | -39.00 |
| T7        | 5.29 | 1.88    | 7.40            | 4.10            | 11.50           | 338.40 | -43.00 |
| T8        | 5.60 | 1.99    | 7.20            | 4.40            | 11.60           | 314.12 | -45.00 |
| T9        | 5.91 | 2.10    | 7.20            | 4.70            | 11.80           | 288.94 | -48.00 |
| T10       | 6.17 | 2.19    | 8.90            | 6.20            | 15.00           | 262.94 | -48.00 |
| T11       | 6.47 | 2.30    | 9.00            | 6.20            | 15.20           | 235.30 | -46.00 |
| T12       | 6.74 | 2.39    | 11.00           | 7.20            | 18.10           | 204.56 | -44.00 |
| L1        | 7.04 | 2.50    | 11.10           | 6.50            | 17.50           | 171.07 | -37.01 |
| L2        | 7.30 | 2.59    | 10.90           | 6.00            | 16.80           | 135.03 | -29.00 |
| L3        | 7.61 | 2.70    | 10.70           | 5.50            | 16.10           | 97.55  | -17.00 |
| L4        | 7.87 | 2.79    | 11.20           | 5.30            | 16.40           | 58.90  | -10.00 |
| L5        | 8.19 | 2.91    | 12.20           | 5.60            | 17.70           | 20.57  | -6.00  |
| S1        | 0.00 | 0.00    | 0.00            | 0.00            | 0.00            | 0.00   | 0.00   |
| Pelvis    | —    | 11.00   | 75.00           | 30.00           | 80.00           | -89.00 | 0.00   |

TM: Trunk Mass, BM: Body Mass,  $I_{xx}$ ,  $I_{yy}$ ,  $I_{zz}$ : mass moment of inertia in anterior-posterior, Transverse and longitudinal directions ( $kg.m^2 (* 10^{-3})$ ), CG-z: height of the centre of mass with respect to the S1 ( $mm$ ), CG-x: anterior-posterior distance from corresponding center of vertebra with negative value indicating an anterior position ( $mm$ ).

unknown muscle forces in the system that exceeds the number of available equilibrium equations. A prescribed segmental rotation at a spinal level generates an equality equation at the same level in the form of  $\sum r_i \times f_i = M$  where  $r$  is the muscle lever arm,  $f$  is the unknown muscle force, and  $M$  is the required moment due to the prescribed rotation.

To resolve the redundancy at each spinal level, an optimization algorithm with the cost function of sum of cubed muscle stresses<sup>22)</sup> is employed. Moreover, inequality equations of unknown muscle forces remaining positive and greater than their passive force components (calculated based on muscle strain and a tension-length relationship<sup>25)</sup>) but smaller than maximum physiological active forces (i.e.,  $0.6 \times$  physiological cross-sectional area<sup>26)</sup>) plus passive force components are considered. At each iteration, the muscle forces are fed back as updated external loads onto the FE model at the vertebral level to which they are attached. The iteration is repeated till convergence is reached. Nonlinear FE analyses are carried out by ABAQUS (Simulia Inc., Providence, RI) while the optimization procedures are analytically solved using an in-house program based on the Lagrange Multipliers Method. Meanwhile, a passive FE model (without musculature) is also considered for comparison and delineation of the role of muscle forces in the dynamic response.

#### Laboratory measurements

In earlier experimental studies, biodynamic responses of seated human body to vertical vibration in terms of force-motion and vibration transmission properties have been mea-

sured<sup>16, 17)</sup>. Those measurements were mainly performed to characterize the role of various parameters, such as the back support condition, hands position and excitation magnitude on the apparent mass (APMS) and seat-to-head transmissibility (STHT) responses.

The experiments were conducted using a rigid seat with a configuration representative of automotive seats. The force-plate at the seat base was fabricated using four Kistler load cells with a summing junction to measure the total driving force acting on the seat base along the z-axis. The seat and the force platform were installed on a vertical WBV simulator. A single-axis accelerometer (Analog Devices Model ADXL05 EM-1) was installed on the simulator to measure the input acceleration. A three-axis accelerometer was used in a light-weight helmet-strap mounting system to acquire the head accelerations along the three translational axes. The vibration simulator was operated using the white-noise vibration spectrum in the 0.5 to 15 Hz frequency range. Three different levels of broad-band excitations were synthesized to yield overall rms acceleration values of 0.25, 0.5 and 1  $m/s^2$ . A total of 12 healthy adult male volunteers were involved in the experiments. Three different back support conditions were considered: (i) sitting with no back support; (ii) sitting with upper body supported against a vertical backrest and (iii) sitting against the inclined backrest (with an inclination angle of 24° with respect to the z axis). Under each back support condition, the subjects were also instructed to assume two different hand positions: hands on laps representing a passenger-like sitting posture and hands on the steering wheel representing

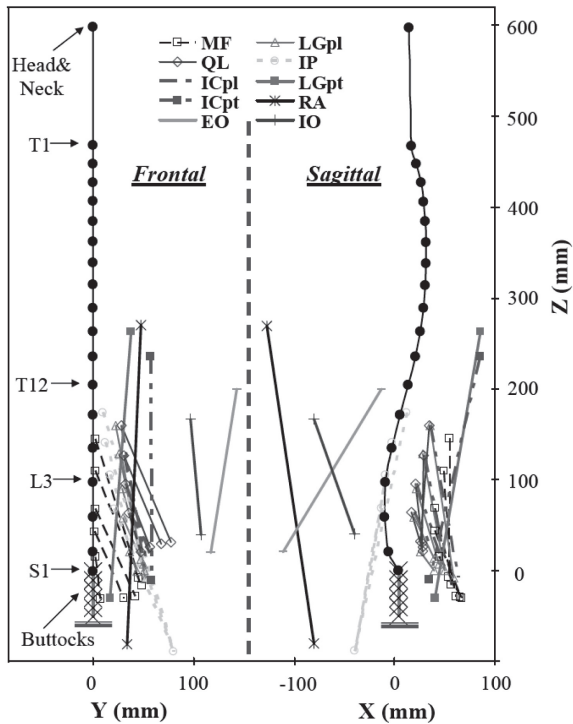


Fig. 2. Spinal global and local musculatures in the sagittal and frontal planes (only fascicles on one side are shown). ICpl: Iliocostalis Lumborum pars lumborum; ICpt: Iliocostalis Lumborum pars thoracic; IP: Iliopsoas; LGpl: Longissimus Thoracis pars lumborum; LGpt: Longissimus Thoracis pars thoracic; MF: Multifidus; QL: Quadratus Lumborum; IO: Internal Oblique; EO: External oblique; and RA: Rectus Abdominus. The positions of mass centres at different levels are listed in Table 1.

the driver-like sitting posture.

The vertical APMS was derived from the spectral analyses of the data, namely, the complex ratio of cross-spectral density between the vertical acceleration and force measured at the seat base, and the auto-spectral density of the vertical seat acceleration:

$$M_v(j\omega) = S_{z_0 F_v}(j\omega) / S_{z_0}(j\omega) \quad (1)$$

where  $M_v(j\omega)$  is referred to as 'vertical APMS' corresponding to the excitation frequency of  $\omega$ ,  $S_{z_0 F_v}(j\omega)$  is the cross-spectral density of the vertical acceleration with the total driving force measured ( $F_v$ ) at the seat base along the vertical  $z$ -axis and  $S_{z_0}$  is the auto spectral density of the acceleration due to vertical seat excitation  $\ddot{z}_0$ .

Similarly, the vertical STHT was derived from the complex ratio of cross-spectral density between the seat acceleration and the vertical head acceleration, and the auto-spectral density of the seat acceleration, such that:

$$T_v(j\omega) = S_{z_0 \ddot{z}}(j\omega) / S_{z_0}(j\omega) \quad (2)$$

where  $T_v(j\omega)$  is referred to as 'vertical STHT' and  $S_{z_0 \ddot{z}}(j\omega)$  is the cross spectral densities of head acceleration along the  $z$ -direction with the vertical seat base acceleration  $\ddot{z}_0$ .

The coherence provides a value ranging from 0 to 1 and

represents the ratio of the square of the absolute value of cross-spectral density to the product of auto-spectral density of the seat and head accelerations for the STHT, the ratio of the square of the absolute value of cross-spectral density to the product of auto-spectral density of the seat acceleration and base force for the apparent mass<sup>28</sup>).

$$\gamma_{STHT}^2 = \frac{|S_{z \ddot{z}_0}(\omega)|^2}{S_z(\omega) S_{z_0}(\omega)} \quad (3)$$

$$\gamma_{APMS}^2 = \frac{|S_{F_v \ddot{z}_0}(\omega)|^2}{S_{F_v}(\omega) S_{z_0}(\omega)} \quad (4)$$

A multi-channel data acquisition and analysis system (Briel & Kjaer Pulse 6.0 system) was employed. The data corresponding to each measurement were acquired over a period of 56 s (25 averages using Hanning window and an overlap of 75%). The data analyses were performed using a bandwidth of 100 Hz and resolution of 0.125 Hz. Each experiment was performed twice, and the results were compared to ensure reasonable repeatability. The coherence response between the forces and accelerations, and force and velocities were constantly monitored during experiments performed to ensure adequate signals<sup>16, 17</sup>. A measurement was rejected when coherence value was observed to be below 0.8 within the entire frequency range. The analyzer software was also programmed to continually display the rms acceleration due to excitation in the third-octave frequency bands which was monitored to ensure consistent excitation.

#### Numerical simulations

Throughout the vibration duration, the a-priori unknown muscle forces are estimated at each time increment using an iterative approach. At each iteration, the penalty of muscle forces in axial and horizontal directions is applied along with the gravity/inertia/external loads on the spine. The procedure is repeated until the convergence is attained; calculated muscle forces in two successive iterations remain almost identical. White noise random vibration in the 0.5–15 Hz range (magnitude=1.0 m/s<sup>2</sup> rms) is considered as input into the model and applied at the buttock–seat interface. The reaction force at the buttock–seat interface and head-T12 acceleration are extracted in the time domain. The force-motion transfer function (APMS) at the buttock–seat interface is estimated using FFT technique and Eq. (1). Similarly, the vibration transmissibility from the seat input to the head-T12 is subsequently computed by Eq. (2) which is considered to represent the vertical STHT.

## Results

The kinematics of the FE model employed in this study (and assumed to remain unchanged during the vibration) represents the posture of a sitting subject with no back support condition and hands on the laps. The remaining sitting postures described in earlier measurements were excluded. The measured data of 10 subjects (body mass = 74.6 ± 3.26 kg) were taken from the ensemble of 12 subjects by eliminating the heaviest and lightest ones. To minimize the inter-subject variations due to body masses, moduli of the apparent

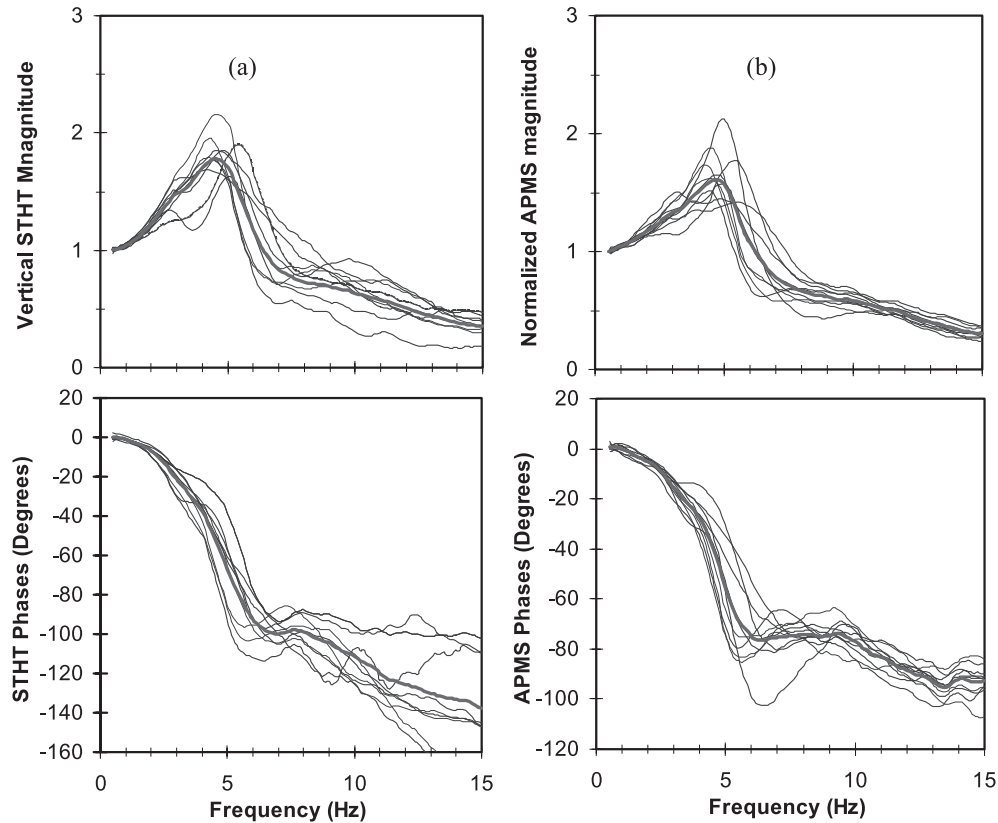


**Fig. 3. Individual and mean biodynamic responses of 10 subjects (thicker lines represent mean curves): (a) STHT transmissibility and phase responses; (b) APMS magnitude and phase responses (no back support and hands on lap sitting posture; excitation at  $1 \text{ m/s}^2$  rms).**

masses were normalized by the mass supported by the seat. Individual magnitude and phase responses of vertical STHT ( $T_v$ ) responses and normalized APMS ( $M_v$ ) responses measured for 10 subjects seated with no back support conditions and hands on laps posture while exposed to  $1 \text{ m/s}^2$  rms acceleration excitation are depicted in Fig. 3. Corresponding mean responses are also indicated (thicker lines). A principal resonance was consistently detected in the range of 4 to 5.5 Hz in both measured apparent mass and seat-to-head transmissibility responses. The mean vertical STHT moduli were noted to be higher than the mean normalized vertical APMS magnitude over the entire frequency range. But the primary resonances taken at the peak magnitudes of both responses were nearly identical, reaching  $4.79 \pm 0.41$  Hz for the APMS and  $4.66 \pm 0.45$  Hz for the STHT.

The STHT and APMS responses of both active and passive FE models are compared with the mean measured responses in Figs. 4 and 5, respectively. The standard deviation of the measured mean is also shown as error bars. The computed results of the active FE model demonstrate a good agreement with the mean measured data in both the APMS and STHT magnitude and phase responses over the frequency range considered. The model responses show primary resonance around 4.5 Hz in both the APMS and STHT. On the contrary, results of the passive FE model lie outside the range of measured data, especially in the neighbourhood of the primary resonance.

Temporal variations of muscle forces and spinal loads at different levels were evaluated in model studies. Large variations in the muscle forces were estimated during the entire base excitation as seen for example in Fig. 6 for a major global extensor muscle, longissimus. Time histories of compressive and shear forces in both active and passive models are compared in Figs. 7 and 8, respectively, at the lowermost L5-S1 level where they reach their maximum values. Compression and shear forces are substantially greater when the muscle recruitment is considered.

## Discussion

The overall biodynamic response of the seated human body subjected to vibration has widely been investigated in terms of driving-point mechanical impedance or apparent mass and seat-to-head transmissibility. These biodynamic responses allow for the understanding of physical responses of the seated body to WBV and serve to formulate more reliable biodynamic models<sup>3, 4</sup>). The apparent mass has the advantage that it can be obtained directly from the measured acceleration and force at the driving-point and allows for necessary corrections to account for the inertia force due to the seat structure in a convenient manner<sup>29</sup>). The APMS based on driving-point measurements alone yields considerably smaller variability among datasets when compared to the STHT datasets<sup>30</sup>). Consequently, the vast majority of earlier studies have focused

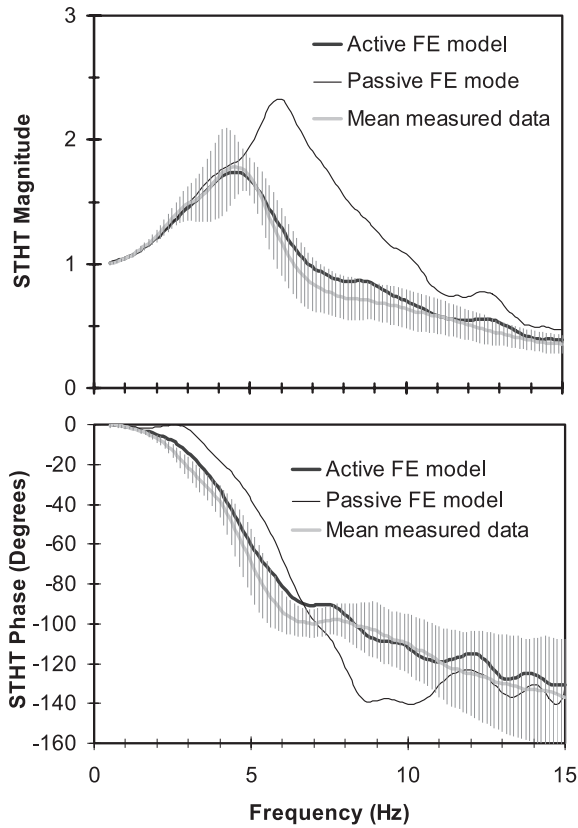


Fig. 4. Comparison of predicted STHT magnitude and phase responses with measured mean  $\pm$  standard deviation responses (no back support and hands on lap sitting posture; excitation at  $1 \text{ m/s}^2$  rms). The passive FE model does not represent muscle activations.

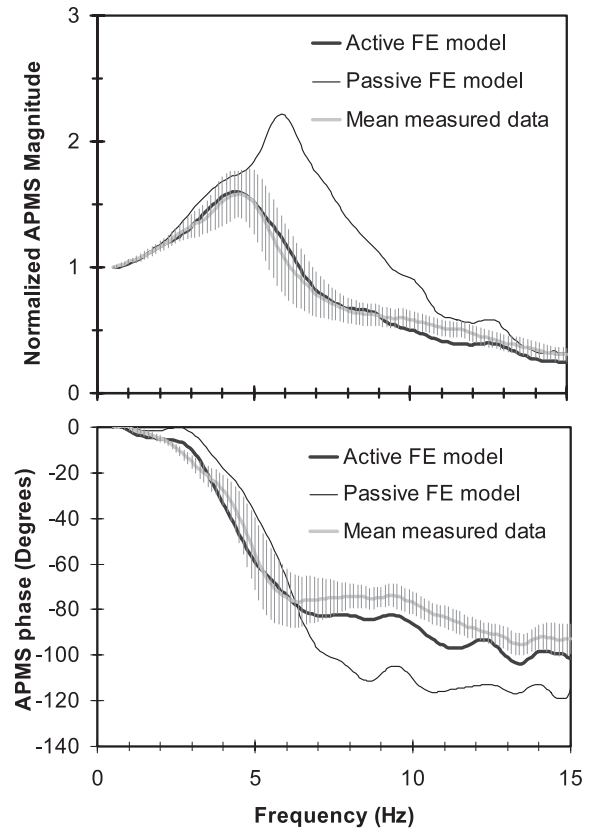


Fig. 5. Comparison of predicted APMS magnitude and phase responses with measured mean  $\pm$  standard deviation responses (No back support and hands on lap sitting posture; excitation at  $1 \text{ m/s}^2$  rms). The passive FE model does not represent muscle activations.

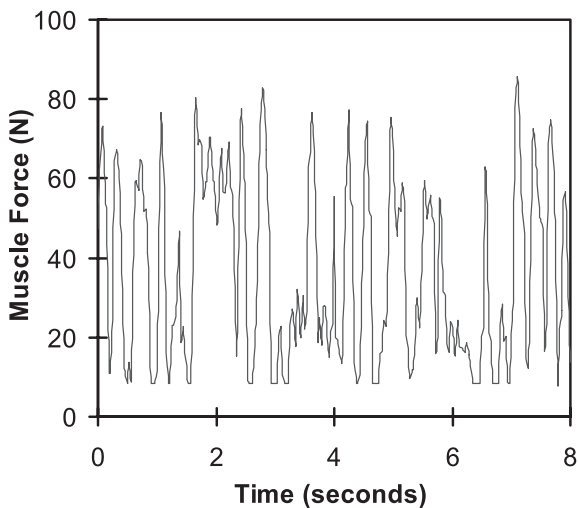


Fig. 6. Temporal variation of predicted force in the global longissimus muscle under the input base excitation in the active FE model.

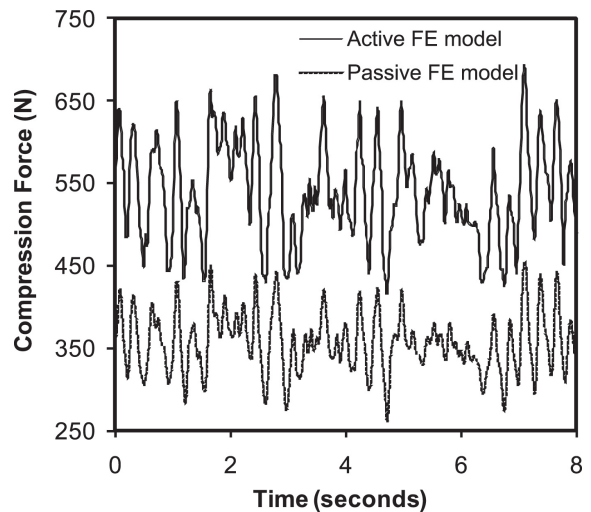


Fig. 7. Comparison of estimated local compression forces in both active and passive FE models at the lowermost lumbar L5-S1 level.

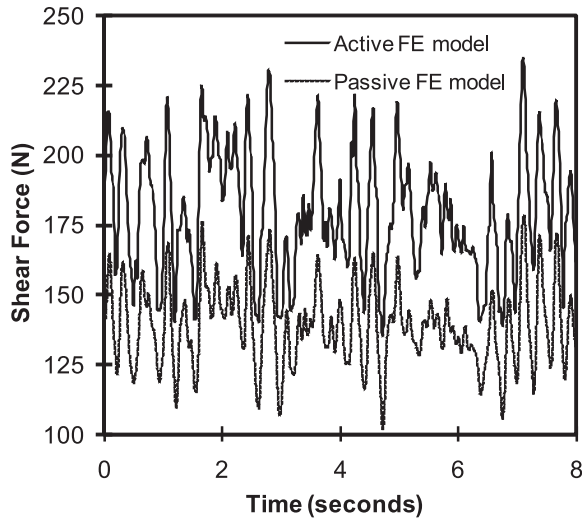


Fig. 8. Comparison of estimated local shear forces in both active and passive FE models at the lowermost lumbar L5-S1 level.

on measurements of APMS responses alone<sup>29, 31-33</sup>). The validation of biodynamic models has often been carried out on the basis of the measured apparent mass responses<sup>29, 32, 35</sup>. The seat-to-head transmissibility likely exhibits larger variations than the apparent mass or impedance between the subjects participating in the same study<sup>9, 36</sup>) due to the concerns with the head motion measurements. For this reason, the use of the seat-to-head transmissibility as the target function has been limited and cautioned<sup>9</sup>).

In previous experimental works, a light-weight strap-mounted accelerometer mounting system has been developed for measurement of head vertical vibration. This measurement method facilitated the adjustment and monitoring of accelerometer orientation while reducing the discomfort caused by a 'bite-bar' system and the inertial force arising from the helmet-mounted measurement systems<sup>16</sup>). This method of head motion measurement is considered to be more reliable. The measured data revealed nonlinearities in the STHT responses and strong effects of back support condition<sup>16</sup>). It was subsequently suggested that both the apparent mass and seat-to-head transmissibility biodynamic responses could provide sound bases for the biodynamic model validation.

Unlike other biodynamic models, the kinematics-driven FE model used in this study included the detailed muscle architecture and considered the time-varying activation of trunk global and local muscles under the WBV. The input kinematics was used to improve computed muscle forces by generating a constraint equation at each level while dealing with the redundant equations separately at various spinal levels. The predictions, hence, satisfied equilibrium at all levels while incorporating nonlinear passive properties of the spine, realistic musculature, trunk dynamic characteristics as well as distributed masses at various levels we prescribed the spinal rotation profiles at different levels and directions based directly on *in vivo* measurements. In the current study and due to lack of direct measurements, however, the prescribed segmental sagittal rotations in both models were assumed to remain unchanged during

the course of vibration. This assumption is reasonable since the participants in the experiments were instructed to maintain their posture and were visually monitored to comply<sup>16, 17</sup>). Minor changes in these rotations during vibration could however slightly influence predictions on muscle forces and spinal loads.

Trunk muscle forces and internal loads of the multi-segment spine are commonly estimated based on the balance of external and internal moments at only one single joint level (e.g., L5-S1). Earlier results suggest that such negligence on equilibrium requirements at remaining levels leads to gross violation of equilibrium at these levels thus yielding incorrect estimations<sup>13</sup>). The responses of the model incorporating active muscle forces revealed satisfactory agreements with the mean measured responses in terms of both the APMS and STHT. The responses of the passive model, however, differed substantially from the mean measured data, which is attributed to the lack of muscle activations in the passive model. The results from this anatomical-based passive FE model thus, in confirmation of our hypothesis, suggest that the activation of muscles in the seated body under WBV exposure contributes considerably to the biodynamic responses.

Comparison of predictions with measurements demonstrates that the results of the passive model without muscle activation cannot match measurements as close as those of the active model. Although using curve fitting-techniques, one can adjust the input material parameters in the passive model or in an idealized lumped-parameter model so as to arrive at estimations that match measured data. Such model parameters, however, do not represent any physiological properties. Moreover, the input data need to be readjusted from one application to another when attempting to simulate different loading, trunk properties, and postural conditions.

The proposed model also estimated the dynamic compression and shear forces acting at different levels of the lumbar spine under WBV. These data would help identify the risk of injury based on cumulative fatigue failure<sup>11</sup>). Such more realistic dynamic FE models are of great help to determine quantities potentially relevant for the evaluation of vibration behaviour and that are not accessible to direct measurements, e.g., internal loads at different levels of the lumbar spine<sup>11, 37</sup>). A few dynamic FE models have been reported in the literature that have overlooked the time-history of muscle forces during the WBV, thus neglecting the effects of dynamic muscle forces on the trunk response. By using iterative kinematics-driven FE approach, the current model yielded results in satisfactory agreements with the measurements and delineated the crucial role of muscle forces.

In summary, an anatomical-based FE model was constructed and validated by comparison with the measured apparent mass and seat-to-head transmissibility biodynamic responses in seated whole body vibrations. By using iterative kinematics-driven FE approach, the current model further revealed the crucial dynamic effects of muscle forces on trunk biodynamic responses. The incorporation of muscle forces led to more realistic physical responses, yielding estimations of biodynamic responses in terms of seat-to-head vibration transmissibility and the apparent mass in close agreement with measured data. Furthermore, the internal shear and compression loads at different spinal levels have been estimated using the FE model.

Muscle recruitments, while needed to maintain trunk equilibrium and stability, substantially increased the loads on the spine and hence the risk of compression failure. The effects of the muscle activity and coactivity on the trunk stability and spinal loads will further be investigated in future works to reveal the likely association between the low-back pain and WBV.

## Acknowledgements

The work is supported by a scholarship from the FQRNT-Québec and a grant from the NSERC-Canada.

## References

- Bovenzi M, Hulshof CTJ (1998) An updated review of epidemiologic studies on the relationship between exposure to whole-body vibration and low back pain. *J Sound Vib* **215**, 595–612.
- Seidel H, Blüthner R, Hinz B, Schust M (1998) On the health risk of the lumbar spine due to whole-body vibration—theoretical approach, experimental data and evaluation of whole-body vibration. *J Sound Vib* **215**, 723–41.
- Boileau P-É, Rakheja S, Yang X, Stiharu I (1997) Comparison of biodynamic response characteristics of various human body models as applied to seated vehicle drivers. *Noise & Vibration Worldwide* **28**, 7–14.
- Liang C-C, Chiang C-F (2006) A study on biodynamic models of seated human subjects exposed to vertical vibration. *Int J Ind Ergon* **36**, 869–90.
- Seidel H, Griffin MJ (2001) Modeling the response of the spinal system to whole-body vibration and repeated shock. *Clin Biomech* **16** (Suppl 1), S3–S7.
- Kitazaki S, Griffin MJ (1997) A modal analysis of whole body vertical vibration, using a finite element model of the human body. *J Sound Vib* **200**, 83–103.
- Pankoke S, Buck B, Wölfel HP (1998) Dynamic FE model of sitting man adjustable to body height, body mass and posture used for calculating internal forces in the lumbar vertebral disks. *J Sound Vib* **215**, 827–39.
- Buck B, Wölfel HP (1998) Dynamic three-dimensional finite element model of a sitting man with a detailed representation of the lumbar spine and muscles. In: *Computer methods in biomechanics and biomedical engineering 2*, Gordon and Breach Science Publishers, London.
- Hinz B, Menzel G, Blüthner R, Seidel H (2001) Transfer functions as a basis for the verification of models – variability and restraints. *Clin Biomech* **16** (Suppl 1), S93–S100.
- Hofmann J, Pankoke S, Wölfel HP (2003) Individualised FE-model of seated humans and representation of motion segments of the lumbar spine as substructure to determine internal loads during vibration excitation, 188, Federal Institute for Occupational Safety and Health, Berlin.
- Seidel H, Hinz B, Hofmann J, Menzel G (2008) Intraspinal forces and health risk caused by whole-body vibration—predictions for European drivers and different field conditions. *Int J Ind Ergon* **38**, 856–67.
- Arjmand N, Shirazi-Adl A, Bazrgari B (2006) Wrapping of trunk thoracic extensor muscles influences muscle forces and spinal loads in lifting tasks. *Clin Biomech* **21**, 668–75.
- Arjmand N, Shirazi-Adl A, Parnianpour M (2007) Trunk biomechanical models based on equilibrium at a single-level violate equilibrium at other levels. *Eur Spine J* **16**, 701–9.
- Bazrgari B, Shirazi-Adl A, Kasra M (2008) Seated whole body vibrations with high-magnitude accelerations—relative roles of inertia and muscle forces. *J Biomech* **41**, 2639–46.
- Bazrgari B, Shirazi-Adl A, Kasra M (2008) Computation of trunk muscle forces, spinal loads and stability in whole-body vibration. *J Sound Vib* **318**, 1334–47.
- Wang W, Rakheja S, Boileau P-É (2006) Effect of back support condition on seat to head transmissibilities of seated occupants under vertical vibration. *J Low Frequency Noise Vibration and Active Control* **4**, 239–59.
- Wang W, Rakheja S, Boileau P-É (2008) Relationship between measured apparent mass and seat-to-head transmissibility responses of seated occupants exposed to vertical vibration. *J Sound Vib* **314**, 907–22.
- Kasra M, Shirazi-Adl A, Drouin G (1992) Dynamics of human lumbar intervertebral joints. Experimental and finite-element investigations. *Spine* **17**, 93–102.
- Pearsall DJ (1994) Segmental inertial properties of the human trunk as determined from computer tomography and magnetic resonance imagery. PhD dissertation. Queen's University, Kingston.
- Bogduk N, Macintosh JE, Pearcy MJ (1992) A universal model of the lumbar back muscles in the upright position. *Spine* **17**, 897–913.
- Stokes IA, Gardner-Morse M (1999) Quantitative anatomy of the lumbar musculature. *J Biomech* **32**, 311–6.
- Shirazi-Adl A, Sadouk S, Parnianpour M, Pop D, El-Rich M (2002) Muscle force evaluation and the role of posture in human lumbar spine under compression. *Euro Spine J* **11**, 519–26.
- El-Rich M, Shirazi-Adl A, Arjmand N (2004) Muscle activity, internal loads and stability of the human spine in standing postures: combined model-in vivo studies. *Spine* **29**, 2633–42.
- Arjmand N, Shirazi-Adl A (2006) Sensitivity of kinematics-based model predictions to optimization criteria in static lifting tasks. *Med Eng Phys* **28**, 504–14.
- Davis J, Kaufman KR, Lieber RL (2003) Correlation between active and passive isometric force and intramuscular pressure in the isolated rabbit tibialis anterior muscle. *J Biomech* **36**, 505–12.
- Gagnon D, Larivie C, Loisel P (2001) Comparative ability of EMG optimisation, and hybrid modelling approaches to predict trunk muscle forces and lumbar spine loading during dynamic sagittal plane lifting. *Clin Biomech* **16**, 359–72.
- Raikova RT, Prilutsky BI (2002) Sensitivity of predicted muscle forces to parameters of the optimization-based human leg model revealed by analytical and numerical analyses. *J Biomech* **34**, 1243–55.
- Bendat JS, Piersol AG (1992) *Random data-analysis and measurement procedures*. John Wiley & Sons, New York.
- Fairley TE, Griffin MJ (1989) The apparent mass of the seated human body: vertical vibration. *J Biomech* **22**, 81–94.
- Boileau P-É, Wu X, Rakheja S (1998) Definition of a range of idealized values to characterize seated body biodynamic response under vertical vibration. *J Sound Vib* **215**, 841–62.
- Seidel H (1996) A contribution to the revision of ISO 5982: mechanical driving point impedance and transmissibility of the human body, Personal communications to A. J. Brammer.
- Rakheja S, Boileau P-É, Stiharu I (2002) Seated occupant apparent mass characteristics under automotive postures and vertical vibration. *J Sound Vib* **253**, 57–75.
- Hinz B, Blüthner R, Menzel G, Rützel S, Seidel H, Wölfel HP (2006) Apparent mass of seated men—determination with single- and multi-axis excitations at different magnitudes. *J Sound Vib* **298**, 788–809.
- Griffin MJ (2001) The validation of biodynamic models. *Clin Biomech* **16** (Suppl 1), 81–92.
- Nawayseh N, Griffin MJ (2009) A model of the vertical apparent mass and the fore-and-aft cross-axis apparent mass of the human body during vertical whole-body vibration. *J Sound Vib* **319**, 719–30.
- Paddan GS, Griffin MJ (1998) A review of the transmission of translational seat vibration to the head. *J Sound Vib* **215**, 863–82.
- Hinz B, Seidel H, Hofmann J, Menzel G (2008) The significance of using anthropometric parameters and postures of European drivers as a database for finite-element models when calculating spinal forces during whole-body vibration exposure. *Int J Ind Ergon* **38**, 816–43.